

Using weather prediction data for simulation of mesoscale atmospheric processes

Andrey A. Bart*, Alexander V. Starchenko

National Research Tomsk State University, 36 Lenin Avenue, Tomsk, 634050, Russian Federation

ABSTRACT

The paper presents an approach to specify initial and boundary conditions from the output data of global model SLAV for mesoscale modelling of atmospheric processes in areas not covered by meteorological observations. From the data and the model equations for a homogeneous atmospheric boundary layer the meteorological and turbulent characteristics of the atmospheric boundary layer are calculated.

Keywords: Atmospheric boundary layer, weather prediction, turbulence

INTRODUCTION

The available data on meteorological conditions and turbulent flows are usually taken into account in mathematical modeling of air pollution in the urban atmosphere. This paper describes an approach to calculate homogeneous meteorological fields and turbulence parameters in the Atmospheric boundary layer (ABL) using global weather prediction data provided an atmospheric model the SLAV [1] developed at the Russian Hydrometeorological Centre, as well as to perform air pollution calculations for small and medium –sized cities using a model of transport of pollutants with chemical reactions [2].

HOMOGENEOUS ATMOSPHERIC BOUNDARY LAYER MODEL

In order to perform interpolation and generate new meteorological data from the global prediction data required for pollution transfer and turbulence diffusion simulations, a one-dimensional steady numerical model of the atmospheric boundary layer is used for detailed calculation of the lower troposphere vertical structure and its turbulence parameters. This model includes the following set of differential equations:

$$\frac{\partial U}{\partial t} = -\frac{\partial}{\partial z} \langle uw \rangle + f \cdot (V - V_g) + \frac{U_s - U}{\tau_s}; \quad (1)$$

$$\frac{\partial V}{\partial t} = -\frac{\partial}{\partial z} \langle vw \rangle - f \cdot (U - U_g) + \frac{V_s - V}{\tau_s}; \quad (2)$$

$$\frac{\partial \Theta}{\partial t} = -\frac{\partial}{\partial z} \langle \theta w \rangle + \frac{\Theta_s - \Theta}{\tau_s}; \quad (3)$$

$$\frac{\partial Q}{\partial t} = -\frac{\partial}{\partial z} \langle qw \rangle + \frac{Q_s - Q}{\tau_s}. \quad (4)$$

Here U and V are the horizontal components of average wind velocity (the vertical component is assumed to negligible $W \approx 0$), u , v and w are the pulsation constituents of the horizontal and vertical velocity components, respectively, Θ and θ are average and pulsation constituents of the potential air temperature, Q and q are average and pulsation constituents of the absolute air humidity, t is time, z is the vertical coordinate, $(U_g, V_g) = 1/\rho f (-\partial p/\partial y, \partial p/\partial x)$ are the geostrophic wind velocity components, $f = 2\Omega \sin \varphi$ is the Coriolis parameter, φ is the geographic latitude of the region under consideration, Ω is the earth angular velocity and $\langle uw \rangle$, $\langle vw \rangle$, $\langle w\theta \rangle$ and $\langle wq \rangle$ are turbulent correlations of the vertical velocity component

pulsations with the horizontal velocity, temperature and humidity component pulsations, respectively. The Ox axis is assumed to be directed to the East, and the Oy axis – to the North.

Initial conditions and profiles of $U_s(t,z)$, $V_s(t,z)$, $\Theta_s(t,z)$ and $Q_s(t,z)$ for equations (1) – (4) can be obtained by processing of the numerical prediction results using the global model. The humidity, potential temperature and horizontal wind velocity component at vertical levels are calculated using the formula from[3]:

$$\bar{\phi}_s(t, z) = \phi_{sound}^*(t, z)[1 - \chi(z)] + \phi_{ground}(t)\chi(z) \min[1, 0; (z/50)^n],$$

where: $\phi_{sound}^*(t, z)$ is an interpolating function based on spline interpolation of numerical prediction vertical data taken as vertical sounding data $\phi_{sound}(z_j)$, ϕ_{ground} are meteorological parameter values at the surface (at 2 m height); n is an atmospheric stratification dependent index ($n = 0$ for $\phi = \Theta, Q$), $\chi(z) = 1 - \min(1, 0; (z/200)^2)$. The terms such as $(\phi_S - \phi)/\tau_S$ are used in the equations to correct the calculated profiles of ϕ , and the synoptic scale values, ϕ_S , are interpolated with respect to time using the formula $\phi_S = \bar{\phi}_{S1} + (\bar{\phi}_{S2} - \bar{\phi}_{S1})(t - t_1)/\tau_S, t \in [t_1, t_2]$, $\bar{\phi}_{S1}, \bar{\phi}_{S2}$ are vertical profiles of ϕ_S at times t_1 and t_2 , respectively, $\phi = U, V, \Theta, Q$. These additional members are proportional to the difference between the calculated value of a meteorological variable and the value obtained from global synoptic weather prediction data at the subject region. τ_s is the frequency of global numerical weather prediction results update.

The calculated profiles $\bar{\phi}_s(t, z)$ are used to specify initial velocity, temperature and humidity distributions.

To complete the system of equations (1)–(4), a three-parameter turbulence model from [4] is applied, which includes transport equations for the turbulence kinetic energy, k , turbulence integral scale, l , and potential temperature turbulence pulsation dispersion $\langle \theta^2 \rangle$:

$$\frac{\partial k}{\partial t} = -\langle uw \rangle \frac{\partial U}{\partial z} - \langle vw \rangle \frac{\partial V}{\partial z} + \frac{g}{\Theta} \langle w\theta \rangle + \frac{\partial}{\partial z} \left(\sigma_e \sqrt{kl} \frac{\partial k}{\partial z} \right) - \frac{C_D k^{\frac{3}{2}}}{l}; \quad (5)$$

$$\frac{\partial l}{\partial t} = C_{l1} \left(-\langle uw \rangle \frac{\partial U}{\partial z} - \langle vw \rangle \frac{\partial V}{\partial z} + \frac{g}{\Theta} \langle w\theta \rangle \right) \frac{l}{k} + \frac{\partial}{\partial z} \left(\sigma_e \sqrt{kl} \frac{\partial l}{\partial z} \right) + C_{l2} \sqrt{k} \left[1 - \left(\frac{l}{\kappa z} \right)^2 \right]; \quad (6)$$

$$\frac{\partial \langle \theta^2 \rangle}{\partial t} = \frac{\partial}{\partial z} \left(C_\theta \sqrt{kl} \frac{\partial \langle \theta^2 \rangle}{\partial z} \right) - 2 \langle w\theta \rangle \frac{\partial \Theta}{\partial z} - 2 \frac{\langle \theta^2 \rangle}{\tau_\theta}. \quad (7)$$

Here $k = (\langle u^2 \rangle + \langle v^2 \rangle + \langle w^2 \rangle) / 2$ is the turbulence kinetic energy, l is the turbulence integral scale, $\sigma_e = 0,54$; $C_{l1} = 0,12$; $C_{l2} = 0,2$; $C_D = 0,19$; $C_\theta = 1,3$; $\alpha_\theta = 0,1$ are numerical coefficients and $\tau = l / C_D \sqrt{k}$ is turbulence pulsation time scale. The momentum $\langle uw \rangle$, $\langle vw \rangle$ and heat $\langle w\theta \rangle$ turbulence fluxes are calculated by means of algebraic relations given in [5].

Close to the underlying surface (in the surface layer), conditions complying with the basic relations of the Monin–Obukhov similarity theory [6] are specified. The boundary conditions at the top boundary are as follows:

$$z = H : \frac{\partial U}{\partial z} = \frac{\partial V}{\partial z} = 0; \frac{\partial k}{\partial z} = 0; \frac{\partial l}{\partial z} = 0; \frac{\partial Q}{\partial z} = 0; \langle \theta^2 \rangle = 0; \quad \frac{\partial \Theta}{\partial z} = \gamma.$$

The Temperature gradient γ at the upper boundary of the atmospheric boundary layer is calculated from numerically predicted atmospheric conditions.

INPUT DATA

The forecast data at ftp-server of the Hydrometeorological Centre are grib files [7] containing the following information on the standard surface and spatial metrological parameters:

- Surface fields: Air temperature (at the height of 2 m); Relative humidity (at the height of 2 m); North and East wind vector components (at the height of 10 m); Pressure (at the height of 2 m); Precipitation accumulated within 6 hours; Pressure at the sea level; Soil humidity.
- Spatial properties: Air temperature; Relative humidity; North and East wind vector components; Geopotential height.

The forecast data are given in a geographical grid: between 49,68° and 63,36° North latitude with a 0,72° spacing and between 80,1° and 97,2° East longitude with a 0,9° spacing and in a vertical irregular grid denser to the surface and corresponding to the following pressure levels: 1000, 925, 850, 700, 500, 400, 300, 250, 200, 150, 100, 70, 50,30, 20, 10 millibars.

DATA TRANSFORMATION STAGES

Data preparation stages are as follows:

1. Extraction of the meteorological parameter from a global meteorological forecast for an urban area;
2. Transition from air temperature to potential temperature, calculation of the geostrophic wind vector components, change of relative air humidity for specific air humidity;
3. Vertical interpolation of the meteorological parameters to calculate the values required at the vertical levels;
4. Calculation of the horizontal wind vector components, potential temperature, specific humidity and turbulence diffusion coefficients using basic the boundary layer equations (1) – (7).
5. Writing the calculated meteorological and turbulence parameters of the atmospheric boundary layer into files to transfer the values to other models and visualization tools.

Advantages of the above described approach are as follows:

1. High degree of elaboration: compared to the measurements at most meteorological stations are taken once every 12 hours, and global forecasts are available with a 3 to 6 hours interval;
2. The global model grid (0.9 ×0.72 deg.) is finer than the meteorological station layout grid in Russia.
3. Remote atmosphere sounding stations are not available at some cities, while global weather forecasts are provided for the whole world;
4. Use of global meteorological forecast data instead of meteorological station measurements allows successful forecasting of urban air quality with no meteorological environment surveillance data network available.

COMPARISON RESULTS

Based on meteorological forecast data provided by the SLAV global circulation model with the above described approach, the following results as shown in Figures 1,2 for October 11, 2012 and October 14, 2012 respectively.

According to measurements taken at the meteorological station Tomsk No. 29430 (56°26'N 84°58'E), on October 11, 2012, the following meteorological conditions were observed [8]: Table 1, Table 2.

Hence, on October 11, the wind speed observed was close to the average seasonal one for autumn in the city of Tomsk (1.2 m/s), on October 14, conditions close to no wind were observed.

Table 1. Observed meteorological conditions, October 11, 2012

Time	Air temperature	Wind direction	Wind speed
10.10.2012 18:00	+0.6°C	W (290°)	1
11.10.2012 0:00	-1.4°C	NW (310°)	2
11.10.2012 6:00	-1.2°C	N (340°)	2
11.10.2012 12:00	+1.2°C	NW (330°)	2
11.10.2012 18:00	+0.4°C		0

Table 2. Observed meteorological conditions, October 14, 2012

Time	Air temperature	Wind direction	Wind speed
13.10.2012 18:00	+0.3°C		0
14.10.2012 0:00	-6.5°C		0
14.10.2012 6:00	-6.6°C		0
14.10.2012 12:00	-4.8°C		0
14.10.2012 18:00	-5.6°C	S (190°)	1

The calculated speed and direction of the surface wind and surface air temperature were compared with measurement data at the TOR-station and Base Experimental Complex (BEC), Laboratory of atmospheric composition climatology, Institute of Atmospheric Optics SB RAS [9]. The figures show calculated results with solid lines, BEC measurement results – with symbol ■ and TOR measurement results – with symbol ●. 0 hours value in the figures stands for 0 hours local time October 11, 2012 and October 14, 2012, respectively.

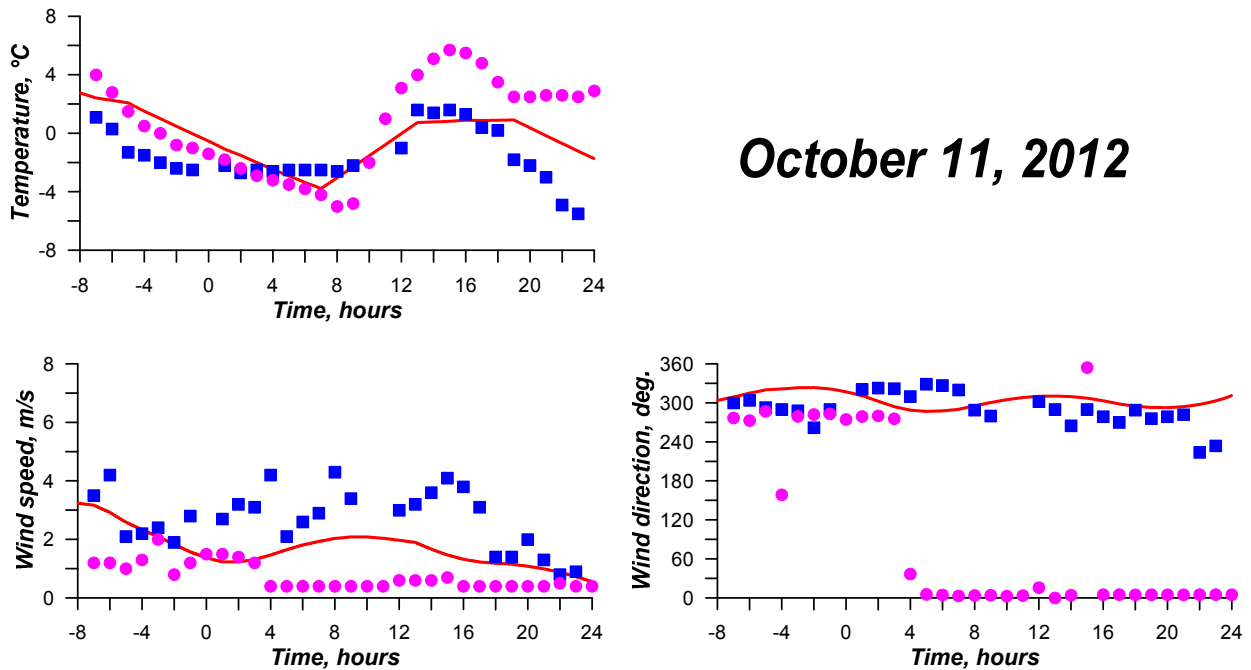


Figure 1. Calculated wind speed & direction and temperature vs the measurement data from TOR-station and Base Experimental Complex on October 10-11, 2012.

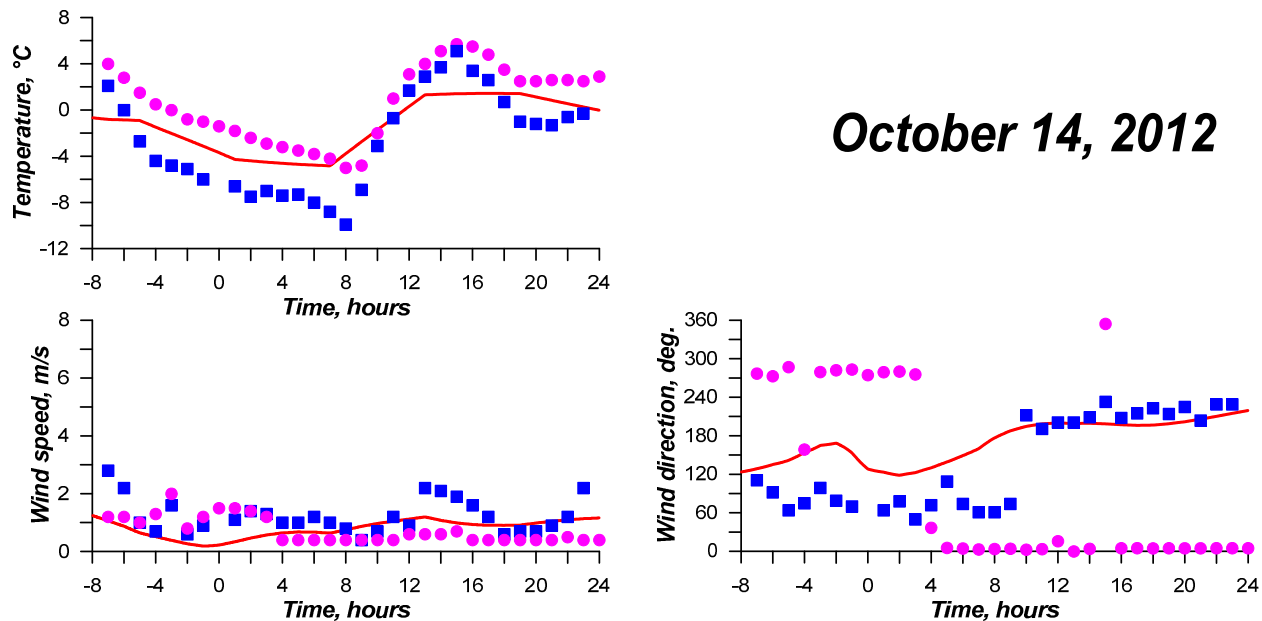


Figure 2. Calculated wind speed & direction and temperature vs the measurement data from TOR-station and Base Experimental Complex on on October 13-14, 2012.

If follows we can see from the figures that the above described approach allows obtaining accurate forecast meteorological parameter values for further use in pollution transfer simulations with chemical reactions. The figures show that the values calculated from the global meteorological forecast correlate better with the BEC measurement data, which can be explained by the fact that the BEC location is with reduced urban influence.

ACKNOWLEDGMENTS

The authors thanks Professor B.D. Belan and the personal of Laboratory of atmospheric composition climatology, Institute of Atmospheric Optics SB RAS for the providing measurement data.

REFERENCES

- [1] Tolstykh, M. A., "Variable resolution global semi-Lagrangian atmospheric model," Russian journal of numerical analysis and mathematical modeling, 18(4), 347-361 (2003).
- [2] Bart, A.A., Starchenko, A.V., Fazliev, A.Z., "Information-computational system for air quality short-range prognosis over territory of Tomsk," Atmospheric and oceanic optics [in Russian], 25(07), 594-601 (2012).
- [3] Kunz, R., Moussiopolos, N., "Simulation of the wind field in Athens using refined boundary conditions," Atmospheric Environment 29(24), 3575-3591 (1995).
- [4] Belikov, D.A., Starchenko, A.V. "Numerical model of turbulent pollutant transport in the atmospheric boundary layer," Atmospheric and oceanic optics 20(8), 607-612 (2007).
- [5] Starchenko, A.V., "Modeling of pollution transport in the atmospheric boundary layer above uniform surface" Proceedings of international conference ENVIROMIS, 77-82 (2000).
- [6] Monin, A. S., Obukhov, A. M., "Osnovnye zakonomernosti turbulentsnogo peremeshivaniya v prizemnom sloe atmosfery (Basic Laws of Turbulent Mixing in the Atmosphere Near the Ground)," Trudy geofiz. inst. AN SSSR 24(151), 163-187 (1954).
- [7] Stackpole, J., "Guide to WMO Binary Code Form GRIB 1", <http://www.wmo.int/pages/prog/www/WDM/Guides/Guide-binary.html> (1994)
- [8] "Russia's Weather - forecast, weather conditions, weather archive", <http://meteo.infospace.ru/>

- [9] Arshinov, M. Yu., Belan, B. D., Davydov, D. K., Ivlev, G. A., Kozlov, A. V., Pestunov, D. A., Pokrovskii, E. V., Tolmachev, G. N., Fofonov, A. V., "Sites for monitoring of greenhouse gases and gases oxidizing the atmosphere," *Atmospheric and oceanic optics* 20(1), 45-53 (2007).